# STEREOLOGICAL ANALYSIS OF ICE FLOW-INDUCED PREFERRED ORIENTATION OF SMALL CLASTS IN TERTIARY TILLITE MATRIX OF MT FEATHER

Piet Stroeven[1], Arjen P. Stroeven[2], Dik H. Dalhuisen[1] and Jaap J.M. van der Meer[3],

[1] Faculty of Civil Engineering and Geosciences, Delft University of Technology, Delft, The Netherlands
[2] Department of Quaternary Research, Stockholm University, Stockholm, Sweden
[3] Geophysics and Soil Mechanics Laboratory, University of Amsterdam, Amsterdam, The Netherlands

## ABSTRACT

The Sirius Group tillite at Mt Feather, McMurdo Dry Valleys, Antarctica, is a deposit of considerable importance to the early glacial history of the Antarctic Ice Sheet. We investigate the power of stereological analysis for an objective determination of the preferred direction of small clasts (< 5 mm) in two cores and, hence, in two core samples drawn at different depths below the tillite surface. Orthogonal sets of vertical thin sections were prepared on this core material. Images measuring 34x22 mm were prepared of 14 sub-areas, jointly representing most of the area of a vertical thin section. From each of these sub-areas, a field of constant 340x340 pp-size was analysed. This involved a systematic line scanning operation, in which the number of intersections between particle traces and the line system was determined. To reduce structural scatter, the resulting 14 roses of the number-of-intersections were averaged per vertical section. These roses reveal the signal coming from the preferred orientation of the clasts to be weak, but above the sensitivity level of the approach. However, this signal is camouflaged by the effect of digitization on the intersection counts, preventing under the present conditions to assess a reliable estimate for the tilt angle of the clasts.

Key words: Antarctica, fabric, line scanning, roses of intersections, texture analysis, tilt angle of clasts.

## INTRODUCTION

The Sirius Group comprises a suite of consolidated deposits, primarily tills, which occur widespread in the Transantarctic Mountains of Antarctica. One of the key outcrops of the currently described 45 locations with Sirius Group sediments (Isaac *et al*, 1996; Stroeven, 1997), is the Sirius Group on Mt Feather (Mayewski, 1972, 1975). This is because of

its extreme location on top of an interfluve, high above surrounding ground, coupled to a vivid discussion regarding the age of deposition based on diatoms reported from this deposit (Harwood, 1983, 1986; Kellogg and Kellogg, 1984; McKelvey *et al.*, 1984; Bleakley, 1996).

On the basis of the age of the youngest marine diatom assemblage, Webb *et al.* (1984) inferred that the East Antarctic Ice Sheet deposited the till, and the marine diatoms they enclose, in the late Pliocene. However, in part based on a reconstruction of the late Pliocene thickening of Taylor Dome (up-ice from Mt Feather), Marchant *et al.* (1993) inferred that the East Antarctic Ice Sheet could not have overridden this mountain at that time. Moreover, Stroeven *et al.* (1996) demonstrated that for nearby Mt Fleming Sirius Group sediments, (i) the sediments were deposited by alpine ice (originating in the mountains nearby) and (ii) that marine diatoms associated to these sediments were derived from atmospheric deposition (Stroeven, 1994, 1996; Stroeven, and Prentice, 1997). Bleakley (1996) and Barrett *et al.* (1997) also found evidence for atmospheric deposition of marine diatoms on Mt Feather. Consequently, for this deposit, they disregarded the imposed age constraints inferred from the assumed glacial transport of marine diatoms. Based on the assumption that the age of preserved (fragile) deposits in valleys down-ice from Mt Feather can constrain the age of overriding, a middle Miocene minimum age has been suggested (*e.g.*, Brady and McKelvey, 1979, 1983; Marchant *et al.*, 1993; Bleakley, 1996).

Mayewski (1972, 1975) first reported on the Mt Feather Sirius Group. Fabric data on more than 50 clasts (long axis 50-150 mm) indicated that deposition was by ice flowing from the east-northeast (Mayewski and Goldthwait, 1985). However, Brady and McKelvey (1979) reported on fabric from which they infer that ice flowed from $325^0$ along a paleovalley that trended $145^0$ (Brady and McKelvey, 1983). Their fabric data is supported by striae trending $145^0$ on 57 clasts embedded in the sediments and by striae trending $145^0$ (3 readings) and $122^0$-$127^0$ (12 readings) on bedrock underlying the till. They also reported on the presence of a deep striation trending $45^0$, which is compatible with the fabric direction from Mayewski and Goldthwait (1985). Finally, Bleakley (1996) reported on fabric data from three locations (totalling 124 clasts) which indicated ice flowing from $352^0$, and postdepositional erosion by ice flowing from the west (based on rat-tail striae of the surface of the till). Consequently, there is ample directional data from multiple studies, strongly indicating that the sediments were deposited by wet-based ice. A recent analysis of microstructures study of Mt Feather Sirius Group samples by van der Meer *et al.* (1998) confirmed this inference.

This paper focusses on determination of the strength of the orientation of small clasts (generally smaller than 5 mm) in the Sirius Group on Mt Feather. Because of the clear macrofabric of this deposit, it was considered worth the effort to seek a similarly clear signal in the preferred orientation direction of microclasts. Van der Meer *et al.* (1998) has detailed the preparation technique of the thin sections from the received dry-cored samples, which were taken at two different depths ($<$ 350 mm and 1400-1650 mm, respectively). The cores were drawn, approximately, in the direction of the earth's axis. However, because the orientation of the core samples relative to magnetic north is unknown, only the strength of the preferred orientation direction of microclasts can be determined, not the former direction of ice flow.

## MODELLING APPROACH TO CLASTS

The tillite layer from which the actual core samples were drawn is simulated by a two-phase system, consisting of a uniform matrix and dispersed non-spherical particles. Although not essential for the experimental assessment of the preferred orientation direction of the clasts, for visualization purposes the particles can be assumed oblong (primarily extending - elongated - in one direction), or oblate (primarily extending - elongated - in two directions). For a system of dispersed **oblong particles** with a preferred orientation, the *orientation axis*, $l$, and the $\{x, y\}$-plane of a Cartesian coordinate system $\{x, y, z\}$ enclose an angle $\alpha$. Hence, a plane exists, which contains both the $z$-axis and $l$. An orthogonal coordinate system $\{s, z\}$ is located in this plane. $\Pi$ is a plane through $l$ perpendicular to the $\{s, z\}$ plane. The $\Pi$- and $\{x, y\}$-planes intersect along the line $m$. Similarly, an *orientation plane*, $\Pi$, can be defined in case of a system of dispersed **oblate particles**. This plane also encloses the angle $\alpha$ with the $\{x, y\}$-plane. So, both types of particles lead to a similar situation, shown in Fig. 1. The $\{x, y\}$-plane is referred to in what follows
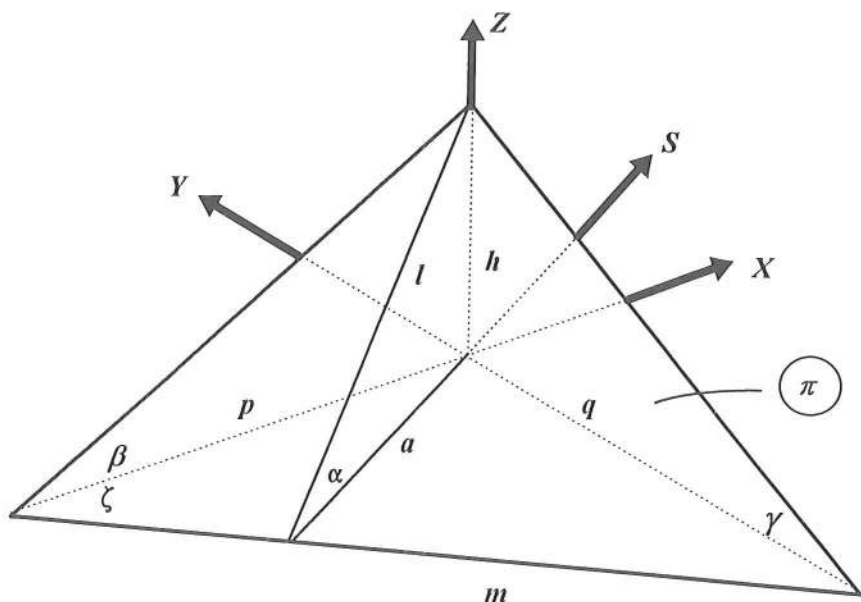


Fig. 1. Assessment of the tilt angle, $\alpha$, in a tillite matrix by line scanning of an orthogonal set of vertical sections yielding information on the preferred orientation angles, $\beta$ and $\gamma$

as the *horizontal* plane, because it approximately corrsponds to a plane perpendicular to the earth's radius at the original core locations. The angle $\alpha$ can therefore be associated with the *inclination* or *tilt* of the small clast.

The orientation in space of an individual oblate or oblong particle is defined by two independent angular parameters, such as $\zeta_i$, $\alpha_i$. The angle $\zeta_i$ is measured in the $\{x, y\}$-plane and the angle $\alpha_i$ in the $\{s, z\}$-plane. $\zeta_i$ and $\sin \alpha_i$ should be conceived as stochastic parameters with average values $\zeta$ and $\sin \alpha$, respectively.

## TEXTURE ANALYSIS BY LINE SCANNING

Texture analysis by line scanning involves coverage of the image plane by a grid of parallel lines, the so called *directed secants*, whereupon the number of intersections with the *traces* of the particle surfaces are counted. The number of intersections is indicated by $P$, and the intersection density by $P/L = P_L$, where $L$ is the total line length of the grid. Perpendicular to the orientation axis of the traces the intersection density will be maximum, while a minimum is found parallel to the orientation axis. It is well-known that the intersection density in a certain direction, $P_L(\theta)$ will equal the total projected length of the traces $(L')$ per unit of area $(A)$, on a line perpendicular to the grid direction, $L'_A(\theta + \frac{\pi}{2})$ (*e.g.*, Stroeven, 1973, 1979). Hence,

$$P_L(\theta) = L'_A(\theta + \frac{\pi}{2}) \tag{1}$$

For the two-dimensional case it is assumed that the actual trace system can be approximated by a mixture of random and oriented line segments, respectively $L(r)$ and $L(o)$. The last one is composed of line elements, which so far will be taken parallel to the horizontal axis. Hence, the angle of preferred orientation is assumed zero. Eq (1) will yield for line scanning operations in the two principal directions (indicated by ' 0' and '$\frac{\pi}{2}$')

$$P_L(0) = P_L(min) = L'_A(\frac{\pi}{2}) \quad = \quad \frac{2}{\pi} L_A(r) \tag{2}$$

$$P_L(\frac{\pi}{2}) = P_L(max) = L'_A(0) \quad = \quad \frac{2}{\pi} L_A(r) + L_A(o) \tag{3}$$

By definition, $L_A = L_A(o) + L_A(r)$, so that combination of eqs (2) and (3) gives

$$P_L(\frac{\pi}{2}) + (\frac{\pi}{2} - 1)P_L(0) = L_A \tag{4}$$

The degree of (planar) orientation in the trace pattern can be defined by

$$\omega_2 = \frac{L_A(o)}{L_A} \tag{5}$$

which upon substitution yields

$$\frac{P_L(\frac{\pi}{2}) - P_L(0)}{P_L(\frac{\pi}{2}) + (\frac{\pi}{2} - 1)P_L(0)} = \omega_2 \tag{6}$$

The present assumption of a partially linear two-dimensional structure implies that the rose of the number of intersections in the image plane has main axes according to eqs (2) and (3), while the radius in an arbitrary direction is given by

$$P_L(\theta) = \frac{2}{\pi} L_A(r) + L_A(o) \sin \theta = P_L(0) + [P_L(\frac{\pi}{2}) - P_L(0)] \sin \theta \tag{7}$$

Herein, $\theta$ is the angle enclosed by the grid system and the 'horizontal' axis.

Derivation of a similar type of equations for the spatial case is equally straightforward. In a first step, the surfaces of the dispersed particles are projected in an arbitrary direction. The total projected area perpendicular to this direction per unit of the specimen volume,

$S_V'(\theta + \pi/2)$ equals the intersection density with the total projected area of a line grid in the projection direction, $P_L(\theta)$. Hence for a mixture of 3-D 'random' surface elements, $S(\text{random})$, and of surface elements oriented parallel to the 'horizontal' plane, $S(\text{oriented})$

$$P_L(0) = S_V'(\frac{\pi}{2}) = \frac{1}{2}S_V(r) \tag{8}$$

$$P_L(\frac{\pi}{2}) = S_V'(0) = \frac{1}{2}S_V(r) + \frac{2}{\pi}S_V(o) \tag{9}$$

The constants, $1/2$ and $2/\pi$, are average projection factors.

By definition, $S_V(o) + S_V(r) = S_V$. Substitution of eqs (8) and (9) yields

$$\frac{\pi}{2}P_L(\frac{\pi}{2}) + (2 - \frac{\pi}{2})P_L(0) = S_V \tag{10}$$

The degree of (spatial) orientation, $\omega_3 = S_V(o)/S_V$, is found upon substitution of the expressions (8) to (10)

$$\frac{\frac{\pi}{2}[P_L(\frac{\pi}{2}) - P_L(0)]}{\frac{\pi}{2}P_L(\frac{\pi}{2}) + (2 - \frac{\pi}{2})P_L(0)} = \omega_3 \tag{11}$$

Hence, planar and spatial quantitative image analysis procedures are similar. Because expressions also have an analogous structure, the spatial approach is selected as the proper one. Determination of $\omega_3$ and of the angles of preferred orientation, $\beta$ and $\gamma$ in the respective sample planes, is accomplished by automatic image analysis procedures. Note that information on $S_V$ will be biased by the filtering process.

Further note, that a similar system of equations can be derived for texture analysis of preferred orientation by means of *total projections*. Ringot (1988) presents an example where this approach is used for crack analysis in concrete.

## ASSESSMENT OF TILT ANGLE

Two arbitrary but mutually orthogonal orientations of the $\{s, z\}$ coordinate system define the $\{x, z\}$-plane and the $\{y, z\}$-plane, which constitute the vertical sections used in the investigations. Photographs of (part of) the image planes were subjected to a sweeping line scanning operation for the construction of the roses-of-intersections. This allows determination of the respective angles of preferred orientation in the plane, $\beta$ and $\gamma$. The situation is sketched in Fig. 1. Herewith, the following relationships are readily obtained

$$\sin \zeta = \frac{a}{p} \tag{12}$$

$$\cos \zeta = \frac{a}{q} \tag{13}$$

$$\tan \beta = \frac{h}{p} \tag{14}$$

$$\tan \gamma = \frac{h}{q} \tag{15}$$

$$\tan \alpha = \frac{h}{a} \tag{16}$$

By combining eqs (12) and (13), it is found that

$$\sin^2 \zeta + \cos^2 \zeta = a^2(\frac{1}{p^2} + \frac{1}{q^2}) \tag{17}$$

Upon substitution of eqs (14) to (16) this yields

$$\tan^2 \alpha = \tan^2 \beta + \tan^2 \gamma \tag{18}$$

In summary, two vertical sections of a sample from both cores were analysed by sweeping test lines to determine the roses of the number of intersections of the surfaces with the dispersed small clast surfaces. The rotation angle of the roses define the respective apparent orientation angles ($\beta$, and $\gamma$). The tilt angle is obtained from the relationship in eq (18).

## AUTOMATIC IMAGE ANALYSIS OPERATION

Images of 14 sub-areas of each of the four vertical thin sections, with a size of 34x22 mm, were scanned and stored on CD. For further elaboration, the scanned (digitized) images (820x520 pp) were employed. Some of the images reveal disturbed areas due to outer edges of the core or of the thin section. Some also have relatively large 'cracked' zones. Therefore, a defect-free area of maximum but constant 340x340 pp size could be defined on most of the images. This was the field subjected to the line scanning operation. All field images were subjected to a software-driven filtering operation, leading to a particulate structure from which the fines were removed. Fig. 2 shows one example of a vertical section's sub-area (of which contrast is somewhat improved), and the field which is subjected to line scanning. To avoid biases by boundaries, all particle sections having their 'lowest' point outside the field were omitted from the texture analysis. Fig. 3 presents the rose-of-the-number-of-intersections obtained in this way. Note that the rose's radii do not start at zero, so differences are exaggerated. The core axis is situated 'vertically'. The analysis of the 14 roses, for each of the vertical sections, are combined for the construction of an 'average' rose to significantly reduce the amount of scatter.

The roses will be approximated by a continuous curve (based on the afore-mentioned concept of a partially-linear system). The orientation of the principal axes provide information on the two-dimensional preferred direction of orientation. The two angular values of preferred 2-D orientation pertaining to an orthogonal set of vertical sections, $\beta$ and $\gamma$, have to be combined according to eq (18) to yield the value of the tilt angle.

## EXPERIMENTAL AND RESULTS

The average roses representing the two sets of vertical sections have been determined from roses such as the one shown in Fig. 2. An example is given in Fig. 4. So far, only the roses of four fields have been used for further analysis. Fig. 4 demonstrates the digitization process to have significantly influenced the intersection counts, i.e. the roses reveal minimum values at the axes and maximum values in oblique directions. The digitization process has increased the trace length of the particle's perimeter in the section plane. The total projected length is of course more favoured by this phenomenon in oblique directions than in those of the principal coordinate axes, as dramatically demonstrated by Fig. 5. In the analysis this bias is accounted for by superimposing (on the partially-linear system) additional 1-D line systems in the two coordinate directions. The analysis of such a partially-oriented multi-linear line system is based on the approach of a partially-linear system, treated in the chapter on *texture analysis and line scanning*.
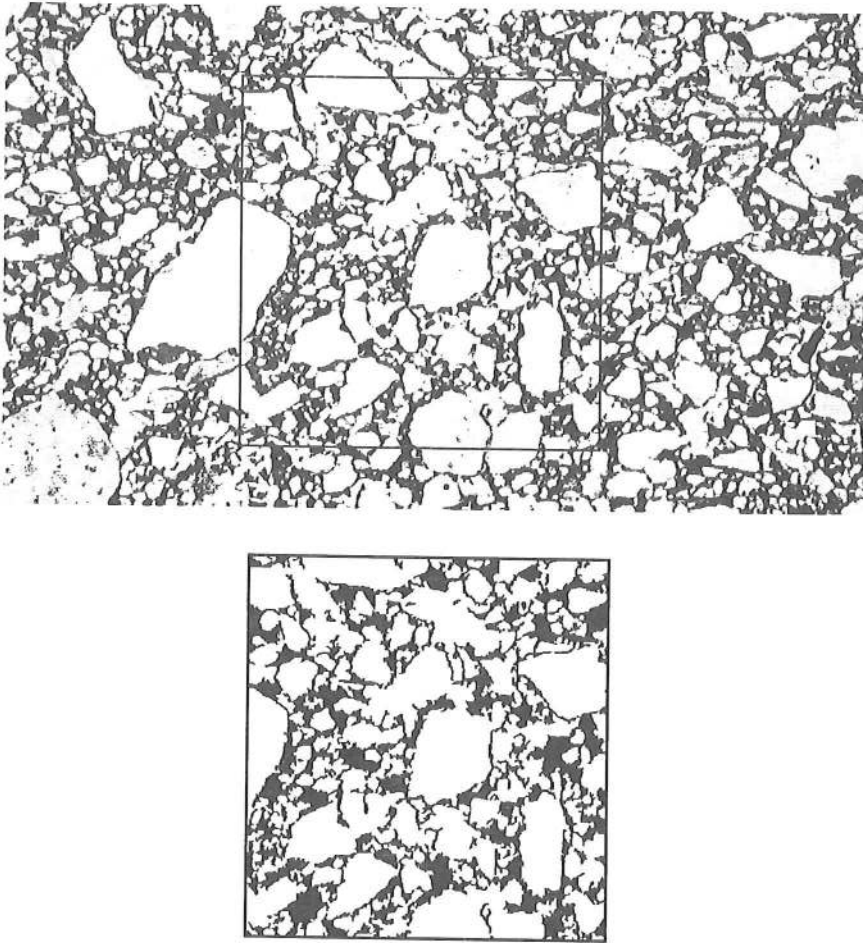
**TR203**



Fig. 2. Image of sub-area number TR 203; the axis of the core is oriented 'vertically'. The field image which is subjected to systematic line scanning is indicated.


## DISCUSSION

Fig. 4 demonstrates the signal to be weak. This also holds for the other roses. The following example may serve to illustrate the relevance of the obtained data. Let $P_L(\theta)$ indicate the intersection density in a direction $\theta$ with the $\{x,y\}$-plane, and let $P_L(d)$ and $P_L(s)$ be the the corresponding values for the digitization effect and the signal related to the tilt of the clasts. The situation is sketched in Fig. 6. It can readily be found that

$$P_L(\theta) = P_L(r) + P_L(d)(\sin\theta + \cos\theta) + P_L(s)\sin(\beta - \theta) \tag{19}$$

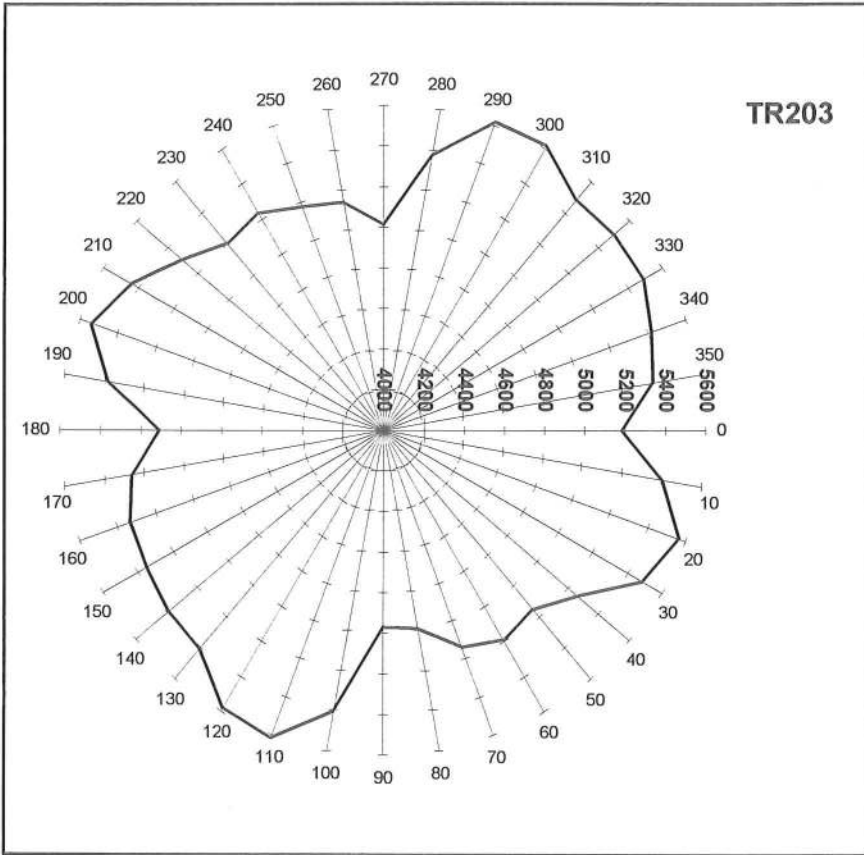Fig. 3. Rose of intersections corresponding to the probed area of Fig. 2

in which $\beta$ is the angle of preferred orientation in the field image. Hence, $\alpha$ should be experimentally determined on the basis of the rose, and $\beta$ estimated by eq (19). After substitution of realistic data, we have

$$P_L(\theta) \sim 3235 + 1270(\sin\theta + \cos\theta) + 250\cos(\beta - \theta) \tag{20}$$

Upon differentiation, the maximum can be found. Hence,

$$1270(\cos\theta - \sin\theta) - 250\sin(\beta - theta) = 0 \tag{21}$$

This can be properly approximated by

$$\tan\theta \sim 1 + 0.2\sqrt{2}\sin(\beta - \frac{\pi}{4}) \tag{22}$$

This allows to draw the conclusion that fluctuation in $\theta$ for the full range of $\beta$-values (0 to $90^0$) is restricted by the digitization effect to a range of about $15^0$ around $45^0$. Hence, sensitivity of the approach is dramatically reduced by the digitization effect. Moreover, the signal is too weak to reveal an obvious optimum in the rose in the indicated range of $\theta$-values, as can be seen in Fig. 4.
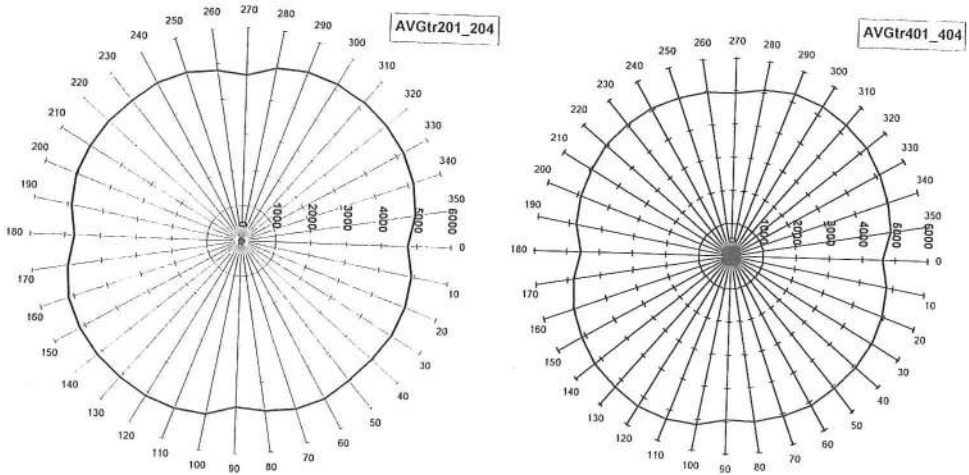
Fig. 4. 'Average' roses based on four fields pertaining to an orthogonal set of thin vertical sections of one core with its axis in 'horizontal' direction.

## CONCLUSIONS

- The presented stereological approach to three-dimensional texture analysis for determination of the possible tilt angle of the clasts is *objective and exact*, and can *readily be automated*, as in the present case. So far, the commonly employed method of texture analysis in the very field consisted of classification of the orientation of individual particles or particle sections, a time-consuming process heavily relying on subjective estimation of the orientation of individual particle sections (Stroeven, 1996). However, this approach is also in vogue outside this field, such as in concrete technology (Karl and Wu, 1970).

- A rough guess of the number, $N$, and volume fraction, $V_V$, of particles involved in the texture analysis process of a single field is 125 and 0.5, respectively. The very dense line system produced recurrent information. For optimum line spacing, where the number of intersections, $P$, would roughly equal the number of particle sections, $N$, an estimate of the variance will be given by: $(1 - V_V)/P = 0.5/125$ (e.g., Stroeven, 1973). The sensitivity is governed by the coefficient of variation of about 6%. After completing the averaging procedure this will decline to about 1.5%. The contribution of the clast orientation effect is of the order of 5%, as in the afore-mentioned example. So, the approach is basically *very sensitive*, and thus able to even detect a weak signal as a tilt angle with low strength.

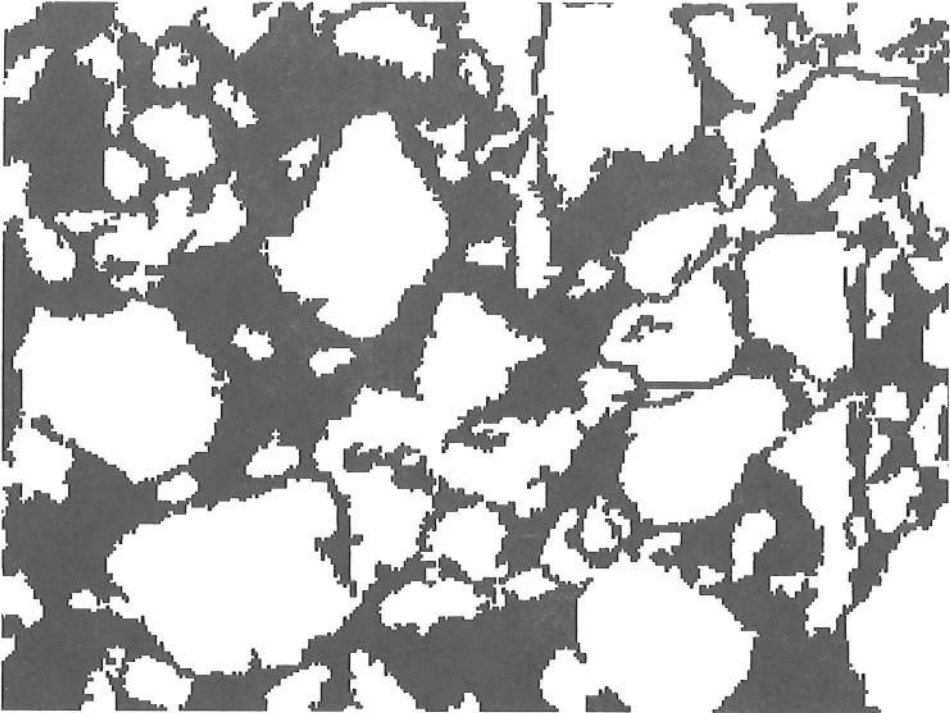- The available system for automatic image analysis has to be adapted for the present

Fig. 5. Magnifigation of part of a field, revealing the influence of digitization on the perimeter of the particle's in the section plane.

situation of an only weakly oriented structure, e.g. the image should be scanned (digitized) in each position in which it is subjected to the line scanning operation. Or, the intersection counting should be performed manually or with a semi-automatic system. This could lead to unbiased detection of low strength signals, as in the present case.

## REFERENCES

Barrett PJ, Bleaky NL, Dickinson WW, Hannah MJ, Harper MA (1997) Distribution of siliceous microfossils on Mt Feather, Antarctica, and the age of the Sirius Group, in Ricci CA, ed, Geological Evololution and Processes, Sienna, Terra Antarctica Publ, pp 763-770.

BleakleyNL (1996) Geology of the Sirius Group at Mount Feather and Table Mountain, South Victoria Land, Antarctica, MSc Thesis: Victoria University of Wellington.

BradyH, McKelvey B (1979) The interpretation of a tertiary tillite at Mount Feather, southern Victoria Land, Antarctica. Journ of Glaciol, 22, 86: 189-193.

BradyH, McKelvey B (1983) Some aspects of the Cenozoic glaciation of southern Victoria Land, Antarctica. Journ of Glaciol, 29, 102: 343-349.

HarwoodDM (1983) Diatoms from the Sirius Formation, Transantarctic Mountains. Antarctic Journ of the US, 18, 5: 98-100.

HarwoodDM (1986) Diatom biostratigraphy and Paleoecology with a Cenozoic history of Antarctic ice sheets, PhD Thesis: Ohio State University.

Isaac MJ, Chinn TJ, Edbrooke SW, Forsyth PJ (1996) Geology of the Olympus Range area, southern Victoria Land, Antarctica (1 sheet + 60 pages), Inst Geol & Nucl Sciences Ltd (1:50.000).

Karl F, Wu M (1970) Gefügeuntersuchungen an Betonen und Discussion des Gefüge-einflusses auf die technischen Eigenschaften. Tonind Zeit, 94, 11: 449-462.

KelloggDE, Kellogg TB (1984) Non-marine diatoms in the Sirius Formation. Antarctic Journ of the US, 19, 5: 44-45.

MarchantDR, Denton GH, Swisher-III CC (1993) Miocene-Pliocene-Pleistocene glacial history of Arena Valley, Quatermain Mountains, Antarctica, Geografiska Annaler, 75A, 4: 269-302.

MayewskiPA (1972) Glacial geology near McMurdo Sound and comparison with the central Transantarctic Mountains. Antarctic Journ of the US, 7, 4: 103-106.

MayewskiPA (1975) Glacial geology and late Cenozoic history of the Transantarctic Mountains, Antarctica. Institute for Polar Studies, Ohio State University, 56.

MayewskiPA, Goldthwait RP (1985) Glacial events in the Transantarctic Mountains: A record of the East Antarctic ice sheet, in Turner MD, Splettstoesser JF, eds., Geology of the Central Transantarctic Mountains: Antarctic Research Series, Washington D.C. Americ Geophys Union, 36: 275-324.

McKelveyBC, Mercer JH, Harwood DM, Stott LD (1984) The Sirius Formation: Further considerations. Antarctic Journ of the US, 19, 5: 42-43.

Ringot E(1988) Automatic quantification of microcracks network by stereological method of total projections in mortars and concrete. Cem Concr Res, 18: 35-43.

StroevenAP (1994) Semi-consolidated glacial deposits on Mt Fleming, South Victoria Land, Antarctica: A test of the late Neogene East Antarctic ice sheet collapse hypothesis, MSc Thesis: University of Maine.

StroevenAP (1996) Late Tertiary glaciations and climate dynamics in Antarctica: Evidence from the Sirius Group, Mount Fleming, Dry Valleys, PhD Thesis: Stockholm University.

Stroeven AP(1997) The Sirius Group of Antarctica: Age and Environments, in Ricci CA, ed, The Antarctic Region: Geological Evolution and processes, Sienna, Terra Antarctica Publ, pp. 747-761.

StroevenAP, Prentice ML (1997) A case for Sirius Group alpine glaciation at Mount Fleming, South Victoria Land, Antarctica: A case against Pliocene East Antarctic ice sheet reduction. Geol Soc of Amer Bull, 109, 7: 825-840.

StroevenAP, Prentice ML, Kleman J (1996) On marine microfossil transport and pathways in Antarctica during the late Neogene: Evidence from the Sirius Group at Mount Fleming. Geol, 24, 8: 727-730.

StroevenP (1973) Some aspects of the micromechanics of concrete, PhD Thesis: Delft University of Technology.

StroevenP (1979) Geometric probability approach to the examination of microcracking in plain concrete. Journ of Mater Sc, 14: 1141-1151.

van der MeerJJM, Hiemstra JF, Stroeven AP (1998) Micromorphology of two Sirius Group core samples from Mt. Feather, Dry Valleys, Antarctica: University of Amsterdam, Rep FGBL-UvA 98/73.

Webb P-N, Harwood DM, McKelvey BC, Mercer JH, Stott LD (1984) Cenozoic marine sedimentation and ice-volume variation on the East Antarctic craton. Geol, 12, 5: 287-291.
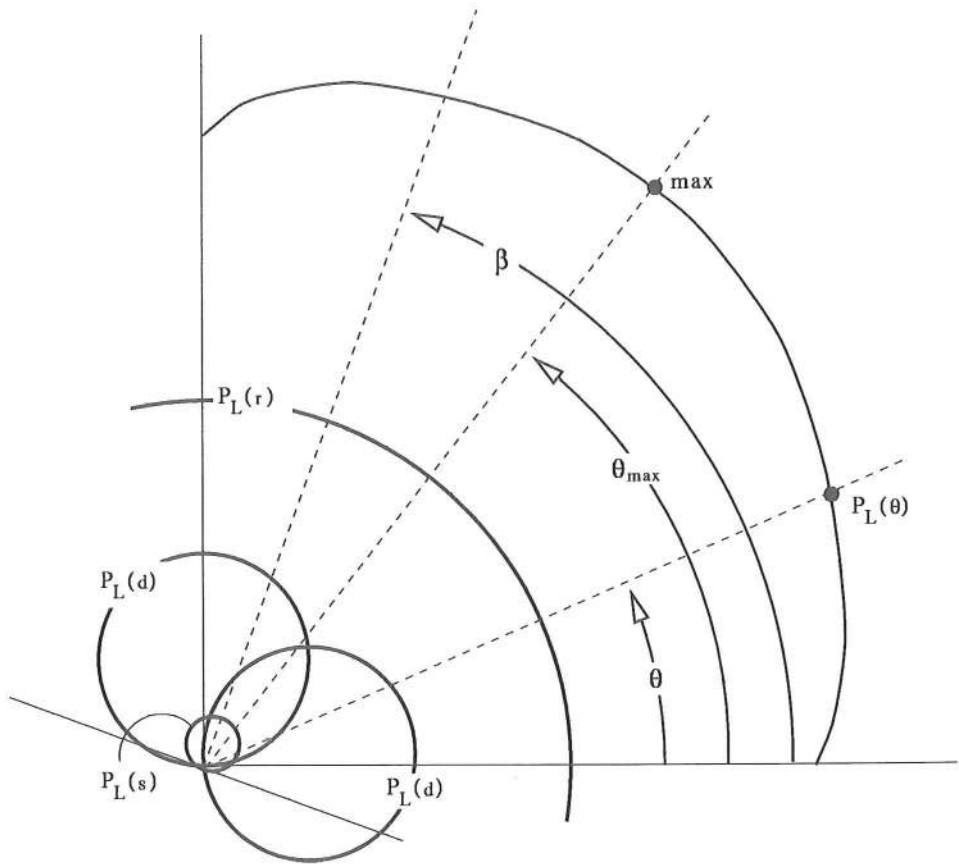
Fig. 6. Model of a partially oriented multi-linear particulate material: construction
of the rose of the number of intersections, $P_L(\theta)$, on the basis of a 2-D random portion,
$P_L(r)$, and contributions by a set of orthogonal line systems resulting from the digitization
process, $P_L(d)$, and the oriented portion stemming from the clasts, $P_L(s)$.